# Hard Extended X-ray Source in the IC 443 SNR Resolved by Chandra:

# A Fast Ejecta Fragment or a New Pulsar Wind Nebula?

A.M. Bykov<sup>1</sup>, F. Bocchino<sup>2</sup>, and G.G. Pavlov<sup>3</sup>

#### ABSTRACT

A Chandra observation of the isolated hard X-ray source XMMU J061804.3+222732, located in the region of apparent interaction of the supernova remnant IC 443 with a molecular cloud, resolved the complex structure of the source in a few bright clumps embedded in an extended emission of a  $\sim 30''$  size. The X-ray spectra of the clumps and the extended emission are dominated by a hard power-law component with a photon index of 1.2–1.4. In addition, we see some indications of an optically thin thermal plasma of a  $\sim 0.3$  keV temperature. The observed X-ray morphology and spectra are consistent with those expected for an isolated supernova ejecta fragment interacting with a dense ambient medium. A possible alternative interpretation is a pulsar wind nebula associated with either IC 443 or another SNR, G189.6+3.3.

Subject headings: ISM: individual (IC 443)—supernova remnants—X-rays: ISM

## 1. Introduction

A substantial fraction of core collapsed supernovae are expected to be spatially correlated with molecular clouds. A well-known example is IC 443 (G189.1+3.0), an evolved SNR of about 45' in size, at a distance of 1.5 kpc (e.g., Fesen & Kirshner 1980). The presence of a molecular cloud at its boundary was established from observations of molecular line emission of OH, CO, and H<sub>2</sub>, excited by a shock (e.g., Burton et al. 1990; Richter et al. 1995). The complex structure of the interaction region, which consists of multiple dense clumps, is clearly seen in the Two Micron All Sky Survey (2MASS) images (Rho et al. 2001). IC 443

<sup>&</sup>lt;sup>1</sup>A.F. Ioffe Institute of Physics and Technology, St. Petersburg, Russia, 194021; byk@astro.ioffe.ru

<sup>&</sup>lt;sup>2</sup>INAF-Osservatorio Astronomico di Palermo, Piazza del Parlamento 1, 90134 Palermo, Italy; bocchino@astropa.unipa.it

<sup>&</sup>lt;sup>3</sup>Pennsylvania State University, 525 Davey Laboratory, University Park, PA 16802; pavlov@astro.psu.edu

is a candidate counterpart of the  $\gamma$ -ray source 3EG J0617+2238 detected with EGRET (Esposito et al. 1996). Large-scale soft X-ray mapping, based on the ROSAT data (Asaoka & Aschenbach 1994), and recent radio observations by Leahy (2004) suggest that another SNR, G189.6+3.3, is possibly seen in the IC 443 field.

IC 443 was observed with HEAO 1 (Petre et al. 1988), Ginga (Wang et al. 1992), ROSAT (Asaoka & Aschenbach 1994), ASCA (Keohane et al. 1997; Kawasaki et al. 2002), BeppoSAX (Preite-Martinez et al. 1999; Bocchino & Bykov 2000), and RXTE (Sturner et al. 2004). The BeppoSAX MECS observations (4–10 keV) identified two compact sources, 1SAX J0617.1+2221 and 1SAX J0618.0+2227, while the BeppoSAX PDS revealed the presence of an unresolved harder component up to 100 keV. Observations of 1SAX J0617.1+2221 with Chandra (Olbert et al. 2001) and XMM-Newton (Bocchino & Bykov 2001) have established the plerionic nature of that source, while the nature of the other source, 1SAX J0618.0+2227, remained unknown.

Bocchino & Bykov (2003; BB03 hereafter) found from the XMM-Newton observations that the hard emission from IC 443 is dominated by 12 isolated sources with fluxes >  $5 \times 10^{-14}$  erg cm<sup>-2</sup> s<sup>-1</sup>. Six of the detected sources are located in a relatively small,  $15' \times 15'$ , region. The analysis of the 2MASS image reveals strong 2.2  $\mu m$  emission indicating interaction with a molecular cloud. The source 1SAX J0618.0+2227, the brightest in this region (excluding the plerion), was resolved with XMM-Newton into two sources. The extended XMMU J061804.3+222732 and the point-like XMMU J061806.4+222832 (we will call them Src 11 and Src 12, respectively, following BB03) have different spectra. The X-ray spectrum of Src 11 is hard (photon index  $\Gamma \lesssim 1.5$ ). Src 12 has a steeper featureless spectrum with  $\Gamma \simeq 2.2$ . To identify the nature of the sources, we observed the field with the Advanced CCD Imaging Spectrometer (ACIS) on board of Chandra.

# 2. Observations and Data Analysis

The field of Src 11 was observed by *Chandra* for 59 ksec on 2004 April 12 (ObsID 4675). The source was imaged at the aim-point on the ACIS-S3 chip. The event files were processed with CIAO tools (ver. 3.1, CALDB 2.28). To account for the extended structure of the source, the redistribution matrix files and weighted auxiliary response files were generated using the CIAO tools *mkrmf* and *mkwarf*.

# 2.1. Imaging

Figure 1 shows  $2'.3 \times 2'.3$  images, centered near the position of Src 11, in three energy bands. The images, presented in a linear scale, are smoothed with a Gaussian kernel of a 2" width. In the soft energy band, 0.3–1 keV, Src 12 (near the top) and Src 11 (at the center) look like point sources. In the 1–3 keV image, in addition to the 0.3–1 keV central source (Src 11a hereafter), we see another compact source, Src 11b,  $\approx$  8" north-north-east of Src 11a, as well as patches of diffuse emission surrounding the two sources. Both Src 11b and the surrounding diffuse emission are also quite prominent in the 3–8 keV image. Thus, the high-resolution *Chandra* images demonstrate that the morphology of Src 11 is rather complex at energies  $\gtrsim$  1 keV, showing bright clumps and structured diffuse emission.

To check whether Src 11a and Src 11b are point-like objects, we extracted their surface brightness profiles and compared with a simulated PSF. The positions of the source centroids were derived using the celldetect algorithm provided by CIAO. They are  $\alpha=6^{\rm h}18^{\rm m}04^{\rm s}32$ ,  $\delta=22^{\circ}27'24''.1$  and  $\alpha=6^{\rm h}18^{\rm m}04^{\rm s}.58$ ,  $\delta=22^{\circ}27'31''.8$  (J2000.0) for Src 11a and Src 11b, respectively. The errors in the derived positions are dominated by the uncertainty in the ACIS absolute position reconstruction,  $\simeq 0''.6$  (90% confidence level). The PSF was simulated with the MARX software (ver. 4.0.8) using the best-fit spectrum derived by the spectral analysis (see §2.2). For Src 11a, we found a significant deviation from the model PSF beyond a 1''.5 radial distance (see Fig. 2), indicating an extended structure of the source. We cannot rule out, however, a possibility that Src 11a is a soft point source embedded in a hard extended halo. For Src 11b, the deviations appear only beyond 3'', so Src 11b resembles a point source on a diffuse background. There is some indication of a third compact source at  $\alpha=6^{\rm h}18^{\rm m}03^{\rm s}.39$ ,  $\delta=22^{\circ}27'29'.5$ , which is visible only in the 1–3 keV band. A deeper exposure is required to examine its properties.

#### 2.2. Spectra

To investigate the nature of the detected sources, we extracted spectra from three regions indicated in the lower panel of Figure 1: Src 11a, Src 11b, and the extended rectangular region R1 in the north-west part of Src 11. For extraction of background spectra, we tested several regions on the ACIS-S3 chip free of point-like and bright diffuse sources. The results were not very sensitive to a particular region choice. The XSPEC package (ver. 11.3) was used to fit the extracted spectra.

The count statistics for the whole region of Src 11 is rather modest (about 1,000 photons collected). The spectral analysis confirms the result of the energy-resolved imaging

Table 1. Fitting parameters for components of Src 11

Parameter	Src 11a	Src 11b	R1
$N_{ m H}$ a	0.7	0.7	0.7
$\Gamma$	$1.3 \pm 0.2$	$1.4 \pm 0.2$	$1.2\pm0.1$
$kT^{\mathrm{b}}$	$0.3 \pm 0.1$	_	_
$F_x{}^{\mathrm{c}}$	21.1	5.2	11.2
$\chi_{\nu}^2/\mathrm{dof^d}$	0.97/17	0.91/4	0.73/17

 $^{\rm a}{\rm Hydrogen}$  column density, in  $10^{22}~{\rm cm}^{-2},$  is fixed in the fits.

 ${}^{\rm b}{\rm Temperature}$  for the  $mekal\,{\rm model}$  component, in keV.

 $^{\rm c} \rm Unabsorbed$  flux in 0.4–7 keV band, in  $10^{-14}$  erg cm  $^{-2}$  s  $^{-1}.$ 

 $^{\rm d} {\rm The\; spectra\; are\; grouped\; to} \ge \! 20$  source coutns per bin.

(Fig. 1) that all the structures within the complex Src 11 contain a hard (power-law) spectral component. Fits of the brightest Src 11a with single-temperature thermal models (optically thin plasma or black-body) are statistically rather poor ( $\chi^2_{\nu} > 1.4$  for 19 dof) or require unrealistic temperatures above 20 keV.

An absorbed power-law model yields statistically acceptable fits for each of the spectra of Src 11a, Src 11b, and R1, with hydrogen column densities  $N_{\rm H}=0.24\pm0.07,\,0.66\pm0.33,\,$  and  $0.94\pm0.33,\,$  respectively (in units of  $10^{22}\,$  cm<sup>-2</sup>; the uncertainties here and in Table 1 correspond to  $1\,\sigma$ ). The  $N_{\rm H}\,$  value for Src 11a is well below the absorption column density  $N_{\rm H}\gtrsim0.7$  for the south-east region of IC 443 obtained with ROSAT (Asaoka & Aschenbach 1994). The XMM-Newton data for the spatially unresolved Src 11 (i.e. for all the three sources combined) gave  $N_{\rm H}=0.63^{+0.21}_{-0.16}\,$  (BB03), similar to the ROSAT fit. We cannot rule out the possibility that Src 11a is less absorbed than Src 11b and R1 because it is a foreground source (e.g., associated with the SNR G189.6+3.3). A more plausible interpretation is that Src 11a, Src 11b, and R1 are physically connected, since a chance probability to find two sources with 2–10 keV fluxes above  $4\times10^{-14}\,$  erg cm<sup>-2</sup> s<sup>-1</sup> (and similar photon indices) within a 7" radius circle in the anti-centre direction is well below  $10^{-3}$ .

If we assume that Src 11a, Src 11b and R1 are at the same distance and fix the column density at  $N_{\rm H}=0.7$ , the power-law model gives acceptable fits for Src 11b and R1, but we have to add an additional soft component for Src 11a (see Fig. 3). Results of such fits, with the additional *mekal* (optically thin thermal plasma emission) component for Src 11a, are presented in Table 1. Such a component is expected if the source is a supersonic ejecta fragment (see §3).

A satisfactory fit can also be obtained if we use a blackbody component, instead of mekal. Such a blackbody + power-law fit, with a temperature of  $\sim 0.1$  keV, radius of  $\sim 3$  km, and power-law index of  $\sim 1.3$  (at fixed  $N_{\rm H}=0.7$ ) can be interpreted as a combination of thermal emission from the surface of a neutron star plus nonthermal emission from the neutron star magnetosphere and/or surrounding pulsar wind nebula (PWN).

It is worth noting that the extrapolation of the hard nonthermal spectrum of Src 11 (see Table 1) into the EGRET range predicts a photon flux similar to that of 3EG J0617+2238, whose position is marginally compatible with that of Src 11. Such a  $\gamma$ -ray luminosity can be expected for both the fragment and PWN interpretations.

#### 3. Discussion

The analysis presented above reveals the complex structure of Src 11, projected onto the region where IC 443 interacts with a molecular cloud. Below we discuss possible identifications of Src 11 with two classes of X-ray objects relevant to SNRs: PWNe and isolated ejecta fragments.

The X-ray source 1SAX J0617.1+2221 in the IC 443 field has been identified by Olbert et al. (2001) and Bocchino & Bykov (2001) as a likely PWN. X-ray-radio morphology and the X-ray spectral steepening toward the outer parts of the nebula support this identification. Recently, Leahy (2004) speculated that this PWN is associated with another SNR, G189.6+3.3, rather than IC 443. The possible presence of two SNRs in the field makes it possible that Src 11 might also be a low-luminosity ( $L_x \sim 10^{32} \text{ erg s}^{-1}$  at 1.5 kpc) PWN, possibly powered by a pulsar in Src 11a that shows a soft thermal-like spectral component. The size ( $\sim 0.2 \text{ pc}$ ), the hard spectrum, and the presence of compact clumps are in agreement with this hypothesis. We found no evidence of spectral steepening in the outskirts of Src 11; however, the count statistics is scarce, and no substantial synchrotron burning is expected in a low radiative efficiency PWN. The complex morphology of Src 11 is rather different from that observed in the 1SAX J0617.1+2221 PWN. However, if Src 11 is indeed inside a molecular cloud, then the PWN appearance can be different from that inside a hot rarefied SNR gas, and, in fact, many PWNe show rather complex morphology in high-resolution images.

Another possible class of compact hard X-ray sources related to SNRs are isolated "knots" associated with fast moving ejecta fragments. A prototype of such objects was observed in the Vela SNR (Aschenbach et al. 1995; Miyata et al. 2001). A massive individual fragment moving supersonically through a molecular cloud would have a luminosity  $L_x \gtrsim 10^{31}$  erg s<sup>-1</sup> in a 1–10 keV band and would be observable with XMM-Newton and Chandra from a few kpc distance.

The model of fast supernova fragments predicts two X-ray emission components (Bykov 2003). The first one is thermal X-ray emission from a hot shocked ambient gas behind the fragment bow shock, with the spectrum of an optically thin thermal shocked plasma of an ISM cloud abundance. A ballistically moving isolated fragment near the boundary of a SNR of age t would have a velocity  $v \sim R/t$ . For the assumed distance to IC 443 of 1.5 kpc and the age  $t \sim 30$  kyr suggested by Chevalier (1999), this estimate gives  $v \sim 250$  km s<sup>-1</sup>. The corresponding post-shock gas temperature is about 0.1 keV, for a standard estimate  $kT = (3/16)\mu m_{\rm H} v^2$ . However, given the uncertainties in the SNR distance and age (e.g., Leahy 2004 suggested that IC 443 is much younger than 30 kyr), post-shock temperatures of about 0.3 keV might be expected as well. Therefore, our detection of the putative thermal

component in the spectrum of Src 11a is in agreement with this interpretation.

The second emission component is nonthermal. Interaction of the fast electrons (accelerated at the fragment bow-shock) with the fragment body produces both hard continuum and X-ray and IR line emission, including the K-shell lines of Si and Fe (Bykov 2002).

We apply the model for X-ray emission from an ejecta fragment of a 0.2 pc size ( $\sim 30''$  at 1.5 kpc, the current size of the fragment) and a mass of  $\gtrsim 10^{-2} M_{\odot}$ , interacting with a molecular cloud (see Bykov 2002, 2003). The knot travels through an inter-clump medium of a number density  $\sim 100~{\rm cm}^{-3}$  with a velocity of  $\sim 500~{\rm km~s}^{-1}$  (corresponding to  $kT \sim 0.3~{\rm keV}$ ). This model predicts a hard continuum with a photon index  $\Gamma \lesssim 1.5~{\rm and}$  a normalization consistent with the observed one (see Table 1). The upper limit on the 1.8 keV Si line flux from the Chandra observation is close to the upper limit  $4 \times 10^{-6}~{\rm ph~cm}^{-2}~{\rm s}^{-1}$  obtained by BB03 with XMM-Newton. To detect or meaningfully constrain the K-shell emission lines of Si and Fe at the level of  $\sim 10^{-6}~{\rm ph~cm}^{-2}~{\rm s}^{-1}$ , expected for a fragment of Src 11 size and velocity, a longer Chandra exposure is required. The Si line would be more suitable for constraining the nature of Src 11 than the Fe line because ACIS is more sensitive around 1.8 keV, and the Si line from IC 443 is not absorbed by the ISM, contrary to the case of SNRs in the Galactic Center region discussed by Bykov (2003).

Note that to reach its apparent position in the molecular cloud, Src 11 must be massive enough,  $\gtrsim 10^{-2} M_{\odot}$ , to overcome strong drag deceleration in the dense matter. The probability of another similarly massive ejecta fragment getting in the ACIS field of view is small. Some of the point-like X-ray sources seen in the cloud and its vicinity could be smaller and less massive,  $\sim 10^{-3} M_{\odot}$ , fragments with luminosities  $L_x \lesssim 10^{31}$  erg s<sup>-1</sup> that are expected to be more numerous. To firmly identify the sources as the fragments, a much deeper observation is required.

The hydrodynamic simulations available (Klein, McKee, & Colella 1994; Wang & Chevalier 2002) predict a complex irregular structure of the fragment body due to the hydrodynamic instabilities. In this case the X-ray image would show an irregular patchy structure, instead of the smooth regular head-tail structure. The patches are due to the emission of dense pieces of the fragmented knot illuminated by the shock-accelerated energetic particles. The bright clumps of a few arcsecond size in Src 11, such as Src 11a and Src 11b, can be explained in that model.

Thus, the morphology, spectra, and X-ray luminosity of Src 11 are generally consistent with those expected for a ballistically moving fragment interacting with a molecular cloud. If confirmed with a deeper exposure, this would provide the first direct evidence of the potentially important class of hard X-ray sources.

Analysis of IR spectra of Src 11 could help to distinguish between a massive ejecta fragment and a PWN. The fragments should be rather numerous in younger SNRs in dense environments (Bykov 2003). In particular, sources similar to Src 11 can substantially contribute to the unusually rich population of hard X-ray sources in the Galactic Center region observed with *Chandra* (Muno et al. 2003). On the other hand, a reliable identification of Src 11 with a PWN, e.g. with high resolution radio observations of Src 11, will be the best test to confirm the reality of the currently putative SNR G189.6+3.3.

Support for this work was provided by the NASA through Chandra Award GO4-5084X and grant NAG5-10865, by RBRF grants 03-02-17433 and 04-02-16595, and by the International Space Science Institute (Bern) through the international teams program.

### REFERENCES

Asaoka, I., & Aschenbach, B. 1994, A&A, 284, 573

Aschenbach, B., Egger, R. & Trümper, J. 1995, Nature, 373, 585

Bocchino, F., & Bykov, A.M. 2000, A&A, 362, L29

Bocchino, F., & Bykov, A.M. 2001, A&A, 376, 248

Bocchino, F., & Bykov, A.M. 2003, A&A, 400, 203 (BB03)

Burton, M.G., et al. 1990, ApJ, 355, 197

Bykov, A.M. 2002, A&A, 390, 327

Bykov, A.M. 2003, A&A, 410, L5

Chevalier, R.A. 1999, ApJ, 511, 798

Fesen, R.A., & Kirshner, R.P. 1980, ApJ, 242, 1023

Kawasaki, M.T. et al. 2002, ApJ, 572, 897

Keohane J.W., et al. 1997, ApJ, 484, 350

Klein, R.I., McKee, C.F., & Colella, P. 1994, ApJ, 420, 213

Leahy, D.A. 2004, AJ, 127, 2277

Miyata, E., Tsunemi, H., Aschenbach, B. & Mori, K. 2001, ApJ, 559, L45

Muno, M.P. et al. 2003, ApJ, 589, 225

Olbert, C.M., Clearfield, C.R., Williams, N.E., Keohane, J.W., & Frail, D.A. 2001, ApJ, 554, L205

Petre, R. et al. 1988, ApJ, 335, 215

Preite-Martinez A., et al. 1999, AIP Conf. Proc. 510, 73

Richter, M.J., Graham, J.R., & Wright, G.S. 1995, ApJ, 454, 277

Rho, J. et al. 2001, ApJ, 547, 885.

Sturner, S., Keohane, J., Reimer, O. 2004, Adv. Sp. Res., 33, 429.

Wang, C-Y., & Chevalier, R.A. 2002, ApJ, 574, 155

This preprint was prepared with the AAS LATEX macros v5.2.

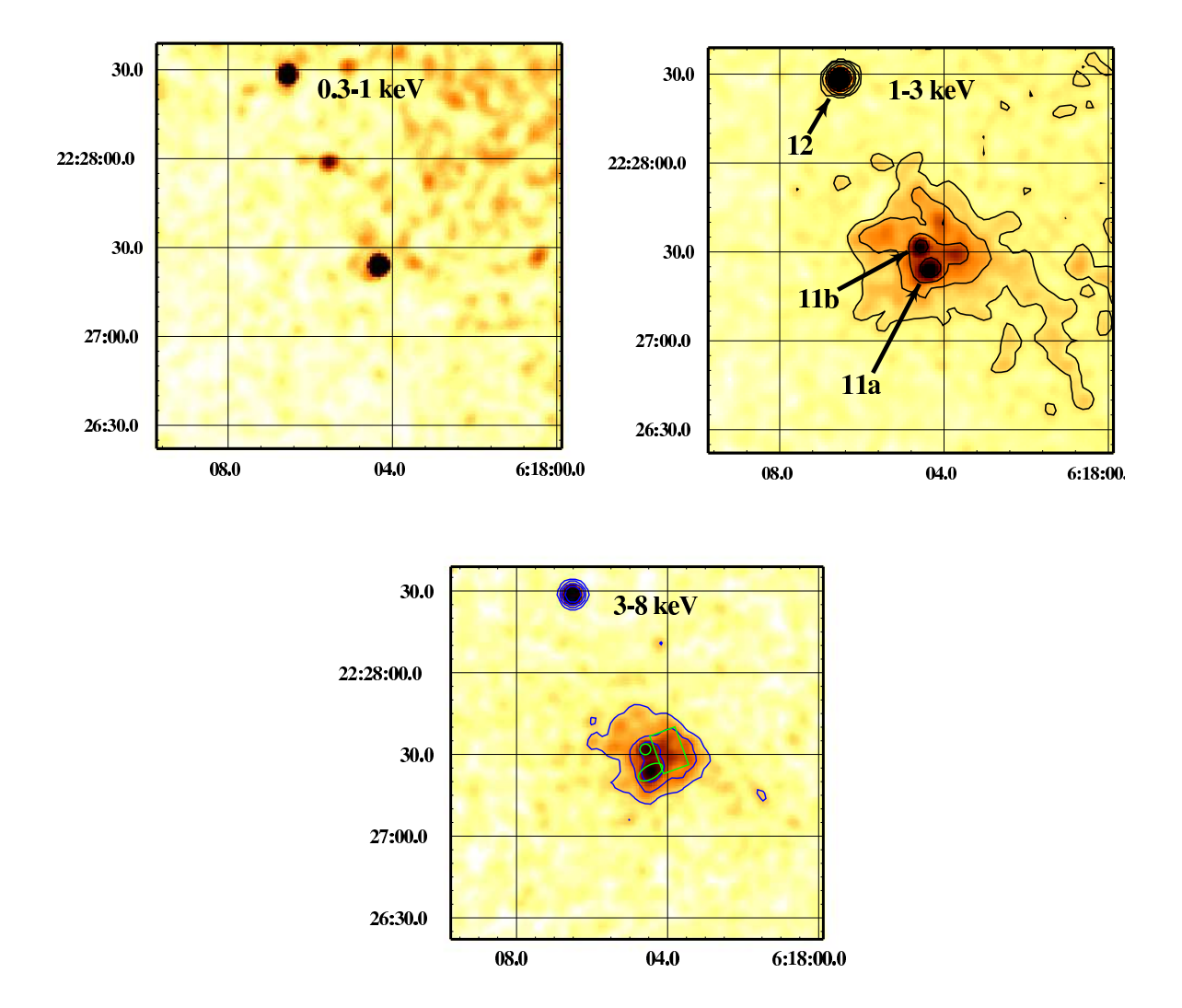


Fig. 1.— *Chandra* ACIS-S3 images of the region of Src 11 in three energy bands. The spectral extraction regions used in spectral analysis are shown in the lower panel.

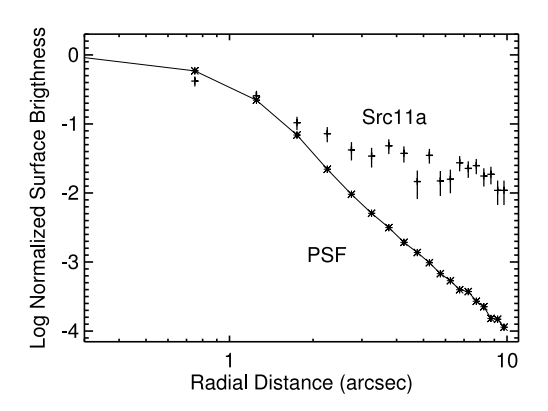


Fig. 2.— Radial brightness distribution for Src 11a in the 1–7 keV band and the PSF model simulated with MARX.

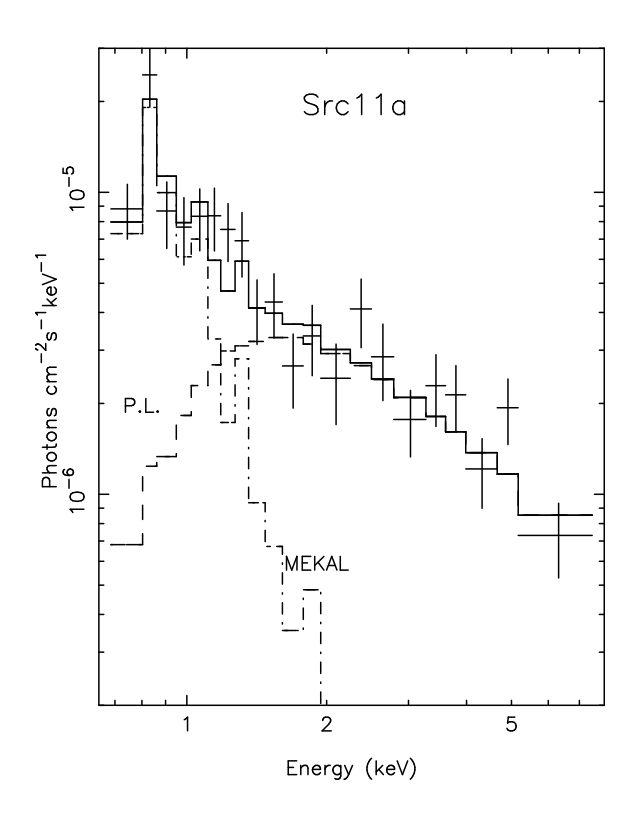


Fig. 3.— Spectral fits to Src 11a: mekal+power-law model (see Table 1).